

Detection of the Process Equipment Components Flaws with the Aid of Thermography

ATEF MAZIOUD¹, JEAN FÉLIX DURASTANT¹, LAURENT IBOS¹, NICOLETA TEODORESCU^{2*}

¹Laboratoire CERTES (EA 3481) IUT of Sénart, Lieusaint, 77127, France

²Politehnica University of Bucharest, Process Equipment Department, 313 Splaiul Independentei, 060042, Bucharest, Romania

The paper presents the problem of the process equipment parts flaw detection with the aid of thermography instead of vibratory analysis. It is presented as an example, a new method (proposed by the authors) of the spalling in rolling-element bearings detection and diagnosis. The idea is to show the existing correlation between the outside temperature of the bearing cap and the vibratory level generated by increasing occurrence of the defect. An experimental study was performed on the test ring which allows the generation, in a progressive manner, of a spalling defect on the external ring of the rolling bearing. On this test rig, simultaneously were measured the mechanical vibration in the radial direction (by means of a piezoelectric accelerometer) and the bearing cap external surface temperature (by means of an infrared camera). The results exhibit a significant correlation between both measures. A detailed study of the heat transfer between the rolling elements and the spalling outside border permits evaluation of the temperature rise due to the heat generated from the defect.

Keywords: *flaws detection, spalling, vibratory analysis, infrared thermography, ball bearing*

The maintenance activity of the industrial installations has been performed for more than twenty years and the diagnosis techniques are increasingly sophisticated. Several techniques of defect detection are available to maintenance engineers today. Among these, we can note infrared thermography for the detection of defects of electrical or mechanical origin; the analysis of lubricants; ultrasound detection; and the measurement of mechanical vibrations.

The process equipment works at very different regime parameters, like high/low pressure and temperature, transitory or steady state loading, with erosive/corrosive fluids etc. [1-9]. The process equipment installations are quite different, and not too easy to be monitored, if there are used methods which need frequent stops, complicated measuring apparatus mounted on them. So it is important, in this case, to adopt the most non-intrusive methods - the best being distance-monitoring. So in the practical maintenance, in general, and in process equipment specially, everyone is looking for the best practices and new measuring/monitoring methods. In the present work one tries to demonstrate that vibration analysis can be successfully replaced by infrared thermography, a very valuable and modern method, best suited for the dynamic loaded process equipment/installations (like mixing devices mounted on large pressure vessels, centrifuges, pumps etc.). A good monitoring of the process equipment means safety functioning and a better preserved environment [9, 10].

The mechanical vibration analysis technique uses signal analysis tools which have seen their field of application widening year after year. One can find in [11] the elements necessary to utilize the classic signal analysis tools, such as: Fourier Transform, Hilbert Transform (for the search of amplitude modulations and/or frequency), as well as the determination of scalar indicators such as: effective value, factor of crest and Kurtosis.

Submitted to radial and/or axial effort which can vary in direction during time, a rolling-element bearing (figure 1) undergoes fatigue under the influence of a variation of load on its rolling elements.

At the end of the 19th century, Hertz [12] established the relations which allow calculation of the constraints and deformations exhibited by two surfaces which run without sliding.

These cutting constraints which affect the rolling elements entail, at the end of a certain number of hours of functioning, a loss of metal from the surface, called spalling. This spalling (fig. 2) can occur a priori on one of the three rolling surfaces (the rolling element, the track of the outside ring, the track of the internal ring).

The spalling will further degenerate, activating the other causes of spalling, and result in the progressive destruction of the rolling-element bearings.

During the passage of the rolling element on the spalling zone, a shock occurs. This impact is repeated periodically. The frequency of the impact repetition depends on the geometry of the rolling-element bearing and on the speeds of rotation.

Vibratory analyses

Many methods are used in signal analysis tools to prevent defects in the rolling-element bearing:

Speed vibration

The vibration is measured in the radial direction with a piezoelectric accelerometer. From this measure, it is calculated the speed of vibration (by integration of the signal), then the effective value of this speed in the frequency interval of 1-10 kHz. We obtain the global level in mm/s.

These measures are compared with the limiting values appearing in the international recommendations as the ISO 10816 standards followed by AB SKF. Arranging the results of the measurement in a sequence in time, it can be

* Tel.: (+40) 0741144647; (+40) 214029360

tracked the evolution of the vibrations and estimates the rolling-element bearing replacement time.

This method yields the first indication of the rolling-element bearing degradation, but is not sufficient for a proper diagnosis.

The crest factor

One can receive earlier warning of the rolling-element bearing defect using the same device as previously, but, in this case, measuring the crest factor at a frequency interval of 1 - 10 kHz. The crest factor, CF , is given by:

$$CF = \frac{A_{crest}}{A_{eff}} \quad (1)$$

where:

A_{crest} is the maximal amplitude of the signal;
 A_{eff} - the effective amplitude of the signal.

At the beginning this ratio is fairly constant. When a localized defect develops, the small resultant shocks increase the level of the crest, but have a weak influence on the effective value. The level of the crest increases until a maximum is reached. When the defect of the rolling-element bearing increases, there are more impacts generated in every passage of the rollings. The effective level thus increases, whereas the level of the crest remains unchanged. In the end of the rolling-element bearing life, the crest factor can fall again to its initial value because the effective value has increased, in its turn.

The major defect of this indicator is to present approximately the same values in both extreme cases (new and end state of life of the rolling-element bearing). Only its evolution is thus significant.

The Kurtosis

The kurtosis technique allows detection of the shocks presence in the measured signal. The greater the kurtosis value, the more is the presence of the significant shocks. As an indication, an absence of shocks gives a kurtosis of 1.5 while this value can rise to several units in a rolling-element bearing exhibiting spalling echo defect. The kurtosis must be calculated after filtering the signal in a range containing a frequency of the defect. The kurtosis is given by the following relation:

$$K = \int_{-x}^x \frac{(x - \bar{x})^4}{\sigma^4} P(x) dx \quad (2)$$

where:

x is the instantaneous amplitude of the signal;

\bar{x} - mean value of x ;

$P(x)$ - probability of appearance of x ;

σ - standard deviation;

Spectrum analysis

It was performed a Fourier transformation on the measured temporary signal to arrive at a frequencies representation, called a 'spectrum'. The shocks in the spectrum are manifested by peaks regularly spaced according to the frequency of the defect (f_{be} , f_{bi} or f_{er}). These peaks will have an amplitude raise closer to the machine frequencies echo. For a first measure, it is advised to choose a wide band (0-20 kHz) to identify well the range of the echo.

Envelope Detection

When these periodic peaks are not clearly visible on the spectrum, one proceeds to a filtering of the signal around a frequency of the echo. After demodulating the filtered signal, can be finally studied the spectrum. The periodic peaks are then more clearly visible.

The manufacturers of rolling-element bearing supply the values of the bearing frequencies. It is sufficient to indicate a reference to the concerned rolling-element bearing and the frequencies of rotation of both ring:

Table 1

N_i (rpm)	N_e (rpm)	f_{be} (Hz)	f_{bi} (Hz)	f_{er} (Hz)
1490.4	0	76.84	121.88	109.96

In table 1 are presented the characteristic frequencies of the spalling defects. N_i is the speed rotation of the internal ring; N_e - the speed rotation of the outside ring;

f_{be} - the impact frequency if spalling is on the outside ring; f_{bi} - impact frequency if spalling is on the internal ring; f_{er} - the impact frequency if spalling is on rolling element,

Remark: these repeated shocks can be expected to induce the machine to vibrate with particular frequencies (frequency of echo).

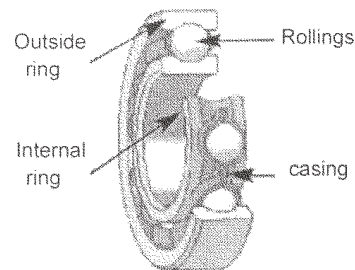


Fig. 1. Rolling bearing

The frequencies generated by the presence of the defect can be calculated with the following formulae:

For the spalling defect situated on the outside ring	$f_{be}(Hz) = \frac{n}{2} f_r \left(1 - \frac{BD}{PD} \cos \beta \right)$	(3)
For the spalling defect situated on the internal ring	$f_{bi}(Hz) = \frac{n}{2} f_r \left(1 + \frac{BD}{PD} \cos \beta \right)$	(4)
For the spalling defect on the rolling element	$f_{er}(Hz) = \frac{PD}{BD} f_r \left[1 - \left(\frac{BD}{PD} \cos \beta \right)^2 \right]$	(5)
For the spalling defect situated on the casing	$f_{be}(Hz) = \frac{n}{2} f_r \left(1 + \frac{BD}{PD} \cos \beta \right)$	(6)

In the equations (3)-(6), there were used the following symbols: n - the number of rolling elements; f - the speed of rotation of the shaft; BD - the diameter of the rolling elements in mm; PD - the diameter primitive of the bearing in mm; β - angle of contact in radians



Fig. 2. Spalling defect

Infrared Thermography

Infrared Thermography carries out measurement of radiation emitted by a scene, with equipment adapted to the conditions in which measurement is carried out, and taking into account the effects of those conditions, to obtain the spatial and temporal distribution of temperatures in the observed scene.

This is a high-performance tool to diagnose any type of heat source, such as:

- electric maintenance;
- buildings;
- furnaces and boilers;
- mechanics and friction;
- fluid problems.

In the present study, the measure of temperature based on infrared thermography allows to detect the presence of abnormally warm zones on the surface of the bearing.

One proposes here to establish a link between the temperature rise and the rise of the vibratory level of a mechanical component during its degradation. The study particularly concerns the detection of the appearance of a spalling defect in a rolling-element bearing [13,14].

The thermography equation

It is important to keep in mind that an infrared camera does not directly measure a surface temperature. The camera sensors respond to the luminance emitted by the studied surface. This luminance is naturally dependent on its surface temperature, although other parameters have an influence.

The equation (7), corresponding to the fundamental equation in infrared thermal imaging, connects the luminance measured to the temperature of the surface studied T_σ

$$L = \tau \varepsilon L^\circ(T_\sigma) + \tau \rho L^\circ(T_{env}) + (1 - \tau) L^\circ(T_a) \quad (7)$$

The measured luminance L contains three terms: a term for emission, a term for reflection considered as an interference and a term arising from the absence of a perfectly transparent atmosphere between the aimed surface and the camera. The notation $L^\circ(T)$ corresponds to the luminance of a body with temperature T considered as a black body, according to Stefan's law:

$$L^\circ(T) = \sigma T^4 \quad (8)$$

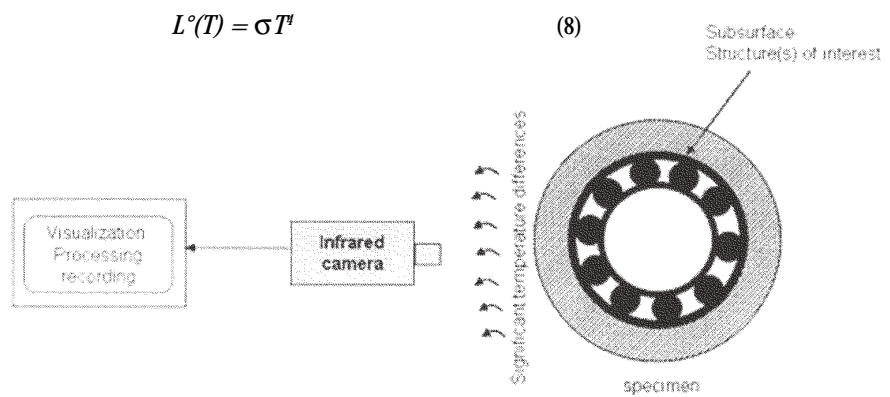


Fig. 3. Schematic setup of infrared thermography for nondestructive testing

where $\sigma = 5.67 \cdot 10^{-8} \text{ W.m}^{-2}\text{K}^{-4}$.

The equation (7) should be written using spectral values, in a given wavelength, λ . To simplify the estimations of the temperature, it is advisable to use total values, on all the band strip wavelengths in which the camera is sensitive. This simplification is based on numerous hypotheses, among which is the fact that observed bodies (solid surfaces and atmosphere) are "grey" in the spectral band of the camera, and their radiative properties are independent of the wavelength.

The relevant emission issuing from the studied surface depends on its surface temperature and also on its emissivity ε . It thus seems clear that inaccurately factoring in the emissivity of the selected surface can generate a significant error in the surface temperature. The term for reflection which "causes" interferences depends on the average temperature of the radiative environment T_{env} and on the factor of reflexion ρ ($\rho = 1 - \varepsilon$ for an opaque surface) of the targeted surface.

The term for the atmosphere emission depends on the temperature of the ambient air T_a , and the factor of transmission τ of the atmosphere in the wavelength spectrum of the camera. The transmittance of the atmosphere also influences the first two terms (appropriate emission and parasite effect) of the equation (7), because a lessening of the luminance emitted or reflected by the wall is observed if the atmosphere between the targeted scene and the camera is not perfectly transparent.

Measuring the luminance L , after correcting the measurement conditions taking into account all the various affected parameters, and calibrating the thermal camera accordingly, one arrives at an accurate measure of the temperature by infrared thermography.

Passive thermography - testing procedure

The first law of thermodynamics concerns the energy conservation principle and states that a significant quantity of the heat is generated by any process consuming energy because of the entropy law [14]. Temperature is thus an essential parameter to measure in order to assess proper operation (fig. 3). In passive thermography, abnormal temperature profiles indicate a potential problem, and a key term is temperature difference with respect to a reference, often referred to as the delta- T (ΔT) value or the hot spot. A ΔT value of a few degrees ($>5^\circ\text{C}$) is generally suspicious, while greater values indicate strong evidences of abnormal behaviour. Generally, passive thermography is rather quantitative since the goal is simply to pinpoint anomalies. However, some investigations provide quantitative measurements if thermal modelling is available, so that measured surface temperature (isotherm) can be related to specific behaviours of subsurface flows.

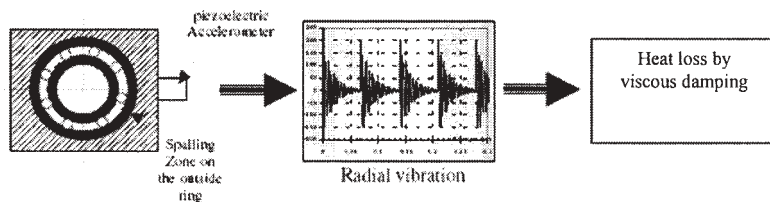


Fig. 4. Rise of temperature of the rolling-element bearing due to the presence of a spalling zone on the outside ring

The advantages of IR camera, with respect to other methods, are that there is no direct contact with the object to be measured and it does not disturb its thermic state. Passive thermography method is a non-intrusive testing procedure.

The measurement methodology

The measurement methodology is described below, in figure 4 (fig. 3).

Periodic impacts are generated by a spalling zone located between one of both rings of the rolling-element bearing (an impact in every passage of a rolling on the spalling zone). These periodic impacts will excite the mechanical system structure (movement, connection with the machine frame etc.). The whole bearing cap will therefore vibrate at its echo frequency. The damping of the vibration has the effect to transform a part of the damping vibratory energy into heat. This heat generation induces a rise in the ring temperature, more particularly on its external surface.

To summarize, one posits that the measurement of this temperature rise could allow the estimation of the vibratory energy quantity generated by the periodic impacts, and therefore the estimation of the rolling degradation level.

The testing platform

The test platform, part of a process equipment installation (fig. 5), allows to rotate a rolling-element bearing with constant motion and adjustable speed of rotation. The main characteristics of the principal testing platform components are:

- AC motor: 1.5 kW, maximum rotating speed 1500 rpm;
- rolling-element bearing type: angular-contact ball bearing (SKF 7206).

Various defaults can be simulated on this test rig. The default analyzed in this paper concerns a spalling on the inner face of the rolling-element bearing.

One can simulate an outside ring defect of the rolling-element bearing by tightening, to a greater or lesser extent, a tightening screw with a radial effort (fig. 6).

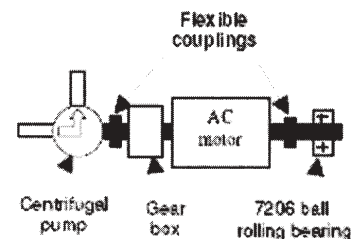


Fig.5. Experimental setup

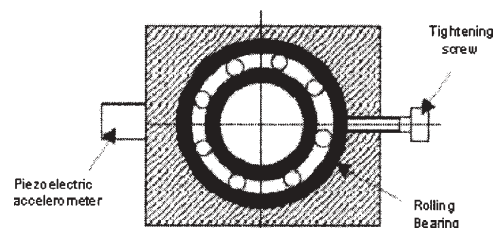


Fig. 6. Experimental setup of defect

An accelerometer measures the vibration in the radial direction. An infrared thermal camera is used to measure the bearing cap exterior surface temperature (fig. 6).

A part of the bearing cap surface of was painted using a high emissivity painting (reference) aiming to eliminate the reflection effect and to reduce the measurement errors.

The rotation speed of the axis is maintained at a constant: 1500 rpm.

For various forces applied by the tightening screw, one measures:

- the vibratory level (effective value in mm/s),
- the external surface temperature of the bearing cap.

The thermal image obtained with the aid of the infrared camera is presented in figure 7.

The obtained correlation between temperature and the vibratory level is presented in figure 8.

As one can see, there is a clear correlation between mechanical and thermal effects.

One established, also, a thermo modeling of the bearing cap of the rolling-element bearing.



Fig. 7. The bearing cap seen by infrared camera

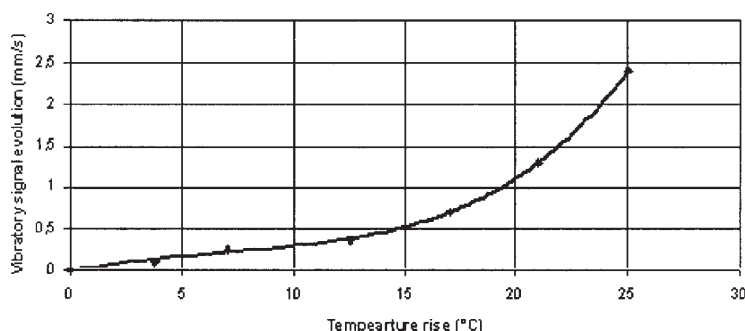


Fig. 8. Evolution of the temperature of the bearing cap according to the vibratory level

Numeric model

The numeric model was meant to determine the temperature field in the rolling-element bearing, the bearing cap and the rotation axis. For this purpose, one used a software program based on the finite volume method [Fluent].

We recall that the presence of an induced defect leads to a characteristic vibratory level transformed into abnormal heating of the system, and thus the heat fluxes generation is added to the nominal heat production. One wishes to verify whether this phenomenon induces a rise of the surface temperature that can be detected by infrared

thermography [14]. So the modeling stage consists in changing the fluxes generated inside the rolling bearing and in measuring the spatial distribution of the temperature.

The modeling hypotheses are the following:

- one assimilates the rollings to a ring;
- one assumes that the contacts between rings and rollings are perfect;
- the rotation speeds of the internal ring and of the rollings are identical;
- heat production is uniform in the ring.

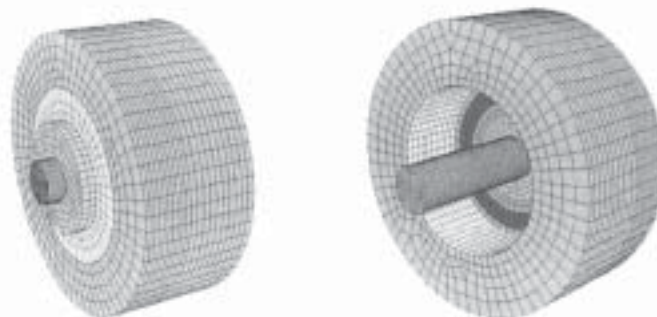


Fig.9. Meshing of the experimental device

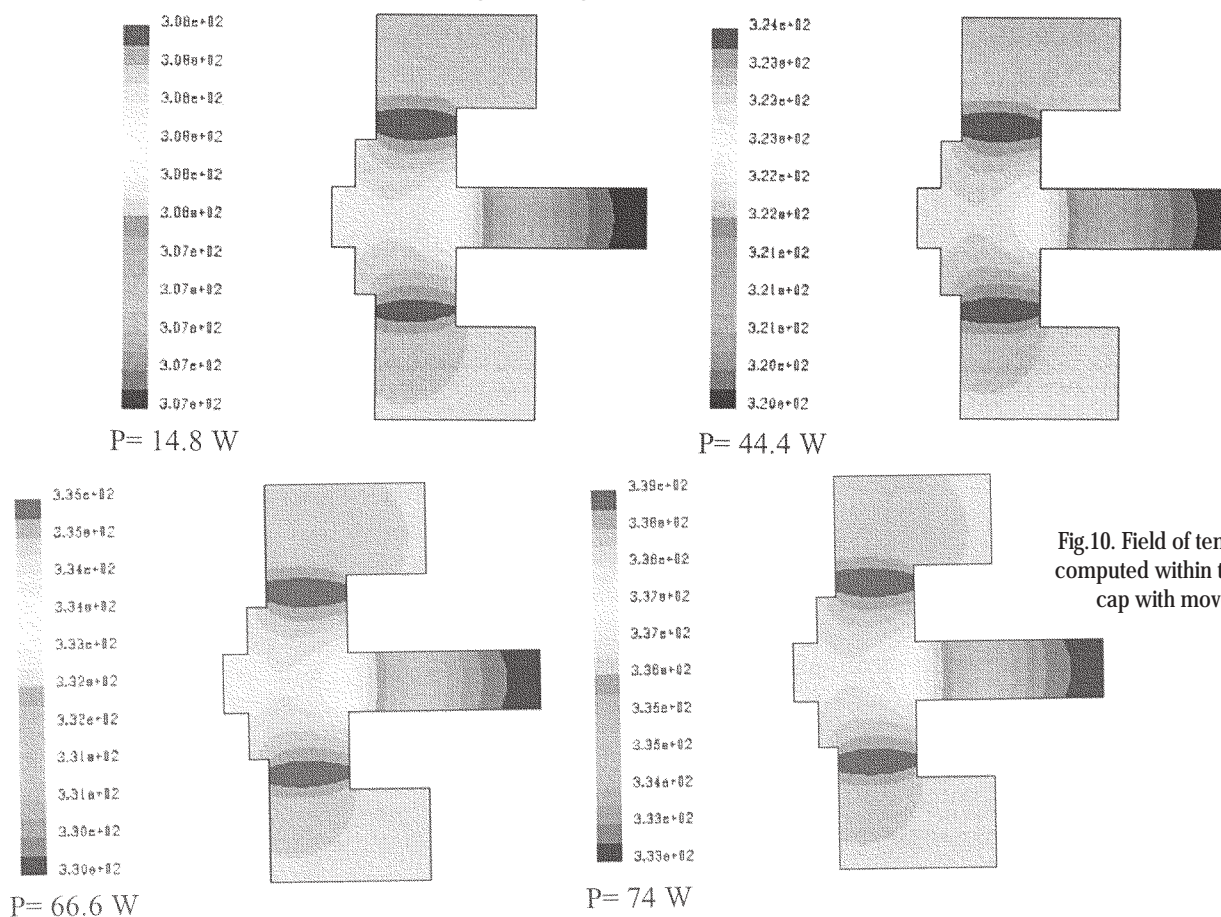


Fig.10. Field of temperatures computed within the bearing cap with movement

In the figure 9 is presented the chosen mesh; it is a three-dimensional structured mesh using parallelepiped cells realized under GAMBIT to optimize the number of cells with the aim to improve the precision and to reduce the computing time; the number of cells is 16079.

The computing conditions are as follows: - ambient temperature: 20°C ; - internal and external side convection exchange coefficients: $10 \text{ W/m}^2/\text{K}$; - convection exchange coefficients on the lower and upper faces: $10 \text{ W/m}^2/\text{K}$; - speed of rotation of the axis: 1500 rpm; - the bearing cap is

made of aluminum with thermal conductivity, $\lambda = 202.4 \text{ W/m. K}$; - the rolling-element bearing and the axis are made of steel with thermal conductivity, $\lambda = 16.27 \text{ W/m. K}$.

Figure 10 presents the temperature field in a section of the experimental device for various values of the power generated inside the rolling-element bearing.

In figure 11, is presented the evolution of the difference ΔT between bearing cap and the ambient temperatures according to the power generated inside the rolling-element bearing.

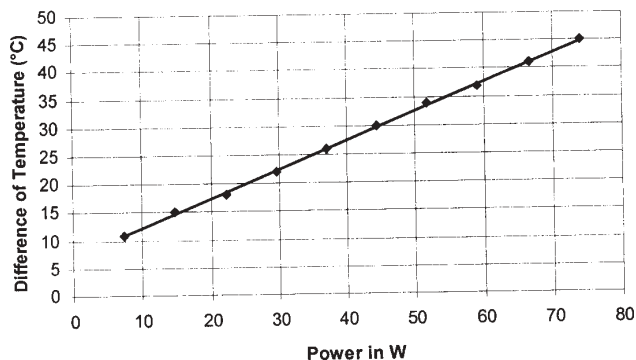


Fig. 11. Calculated evolution of ΔT as a function of the power dissipated by the rolling bearing

As one could expect, the evolution of ΔT is proportional to the power dissipated by the heat source. The slope coefficient is equal to $0.51^{\circ}\text{C}/\text{W}$.

Conclusion

The first results obtained are encouraging. Indeed, on the one hand the vibratory defect engendered within the rolling-element bearing leads to a quantifiable heating of the surface; on the other hand, the numeric model highlights a correlation between vibratory defect and heat production but also allows quantifying the fluxes involved. This research needs to be continued along two directions. A mechanical model should be completed for the analysis

of the mechanical phenomenon to predict heat generation from the defect characteristics. Also, the thermal model can be improved taking into account other parameters, such as the contact resistances between the various mobile parts of the rolling-element bearing.

References

1. JINESCU V.V., PĂUNESCU M., Rev. Chim. (Bucure^oti), **25**, nr. 3, 1974, p. 217
2. JINESCU V.V., PĂUNESCU M., Rev. Chim. (Bucure^oti), **25**, nr. 8, 1974, p. 648
3. JINESCU V.V., PĂUNESCU M., Rev. Chim. (Bucure^oti), **26**, nr. 7, 1975, p. 582
4. JINESCU V.V., Rev. Chim. (Bucure^oti), **26**, nr. 9, 1975, p. 751
5. JINESCU V.V., TACĂ D. Rev. Chim. (Bucure^oti), **44**, nr. 9, 1993, p. 838
6. Pavel A. Revista de Chimie, **32**, nr. 1, 1981, p.71
7. PAVEL A., Rev. Chim. (Bucure^oti), **32**, nr. 2, 1981, p.176
8. PAVEL A., Rev. Chim. (Bucure^oti), **38**, nr. 10, 1987, p.922
9. PAVEL A., Rev. Chim. (Bucure^oti), **44**, nr. 3, 1993, p.256
10. PAVEL A., Revista de Chimie, **44**, nr. 1, 1993, p.368
11. A. BOULENGER, C. PACHAUD, Analyse vibratoire en maintenance préventive, DUNOD, 2003
12. HERTZ H., On the Contact of Rigid Elastic Solids and on Hardness, Miscellaneous Papers, Mac-Millan, London, 1896
13. PADJANI, D., Mesure par thermographie infrarouge, ADD, 1989
14. MALDAGUE X., Theory and practice of infrared technology for nondestructive testing, edition WILEY-INTERSCIENCE, 2001

Manuscript received: 11.02.2008